Journal of Materials Chemistry A

Effects of Surface Chemical Potentials on Cation Segregation

Journal:	*Journal of Materials Chemistry A*
Manuscript ID	TA-ART-09-2020-008850.R1
Article Type:	Paper
Date Submitted by the Author:	23-Nov-2020
Complete List of Authors:	Ostrovskiy, Yevgeniy; University of Maryland at College Park, Materials Science and Engineering Huang, Yi-Lin; University of Maryland at College Park, Materials Science and Engineering Wachsman, Eric; University of Maryland at College Park, Materials Science and Eng. & Maryland Energy Innovation Institute

Effects of Surface Chemical Potentials on Cation Segregation

Eugene Ostrovskiy, [a,b] Yi-Lin Huang,[a,b*] Eric D. Wachsman[a,b*]

[a]Maryland Energy Innovation Institute, University of Maryland, College Park, MD, 20742
[b]Department of Materials Science & Engineering, University of Maryland, College Park, MD, 20742

*Corresponding author email: yilin@umd.edu; ewach@umd.edu

Abstract

Surface cation segregation on perovskite-type electrodes is one of the major issues limiting the durability of high-temperature solid-oxide electrochemical cells, and this process is strongly dependent on temperature, the external gas-environment, and impurities in air, such as CO_2. Here cation segregation on $La_{0.6}Sr_{0.4}Co_{0.2}Fe_{0.8}O_{3-\delta}$ (LSCF) is systematically evaluated under a set of chemical potentials to determine the origin of surface segregation and the dominant factors that govern the segregation process. Temperature is the main driving force for surface strontium segregation as the thermodynamic stability of each phase varies, and the SrO particles appear primarily in a specific operating window. In addition to the required thermal energy, the presence of gaseous oxygen-containing molecules as reactants help drive the precipitation of SrO. Oxygen partial pressure (pO_2) controls the defect chemistry of LSCF, leading to promotion or suppression of surface segregation. The presence of CO_2 promotes the nucleation process and suppresses the surface migration step, significantly altering the surface morphology. We also show that A-site deficiency can limit the SrO segregation in certain conditions but shows no effect in others. This study reveals the impact of gas-solid interactions on surface segregation and highlights the subtle relationship between multiple segregation driving forces.

Keywords: LSCF; Cation Segregation; Degradation: Driving Force; thermodynamics; kinetics

Introduction

Perovskites are widely used for high temperature electrochemical conversion applications such as solid oxide fuel cells (SOFCs) and oxygen permeation membranes, because of their high oxygen activity, conductivity, and tunable nature.[1–3] Generally, multiple dopants are used in both A and B sites of ABO_3 perovskites to achieve desired properties. However, their high oxygen activity toward gas-solid reactions simultaneously causes stability issues after long-term operation at high temperature, mainly cation segregation. $La_{0.6}Sr_{0.4}Co_{0.2}Fe_{0.8}O_{3-\delta}$ (LSCF), one of the most commonly used SOFC cathodes and the most representative case for this degradation mechanism, along with similar Sr-doped perovskite cathodes,[4–6] are susceptible to Sr ion diffusion to the cathode surface as a primary source of degradation. Once the insulating SrO phase is formed on the surface, it blocks active sites and impedes electron conduction.[7–10] This atomic migration occurs during SOFC operation and degrades the performance.[11] Cation segregation has been shown to be a significantly greater problem than other degradation mechanisms such microstructural changes.[12–18] A gas impurity in air, namely CO_2, is also shown to cause degradation issues for perovskite materials.[19–21] Understanding the surface cation segregation mechanism is critical to mitigating the degradation process.

Intensive research has been conducted regarding strontium segregation on LSCF. Studies on the driving force for Sr-segregation suggest that lattice strain between cations (elastic energy) and surface charge (electrostatic energy) are responsible, but the exact mechanisms are difficult to ascertain.[22–26] The composition of the A and B-sites of perovskites, as well as oxygen non-stoichiometry, is found to affect Sr-segregation.[24] Previous work showed the effects of oxygen partial pressure (pO_2), moisture, and mechanical strain on cation segregation process.[7,25,27,28] However, the temperature and pO_2 range in previous studies were performed only in a small

window. Thus, proposed mechanisms based on limited testing conditions might not fully represent the full situation. At high-temperature, the gas-solid interactions between gaseous molecules and the solid surface are expected to strongly influence surface chemistry of these perovskites, but the driving force for segregation and the influence of gas environment is rarely discussed. How pO_2 and carbon dioxide partial pressure (pCO_2) mutually affect the surface cation segregation process is still unclear. Moreover, since the gas environment and the strain are considered as the major causes of cation segregation, testing conditions (ambient, vacuum) and samples preparation (especially in the case of thin film studies) would likely affect the results.[9,29–31]

Here the surface cation segregation of LSCF is systematically studied over a wide range of conditions that resemble SOFC operation to elucidate the fundamental surface segregation mechanism and the dominant governing factors for these segregation processes. Instead of using thin films, we decide to monitor the segregation process on bulk LSCF so that our observation might not be affected by the substrate lattice strain. Dense, polished LSCF samples were aged in a controlled environment to carefully explore the roles of temperature, time, gas compositions on surface segregation. Our results show that there is a specific window of temperature and pO_2 that facilitates SrO segregation. Also, we demonstrate how the gas environment, such as CO_2 concentration, directly impacts the segregation process and cross-reference our findings with the proposed driving forces in the literature.

Results and Discussion

Operating temperature is a primary contributor to the thermodynamic stability of the LSCF surface and can be used to understand the growth conditions for Sr-based secondary phases in addition to its cause. **Figure 1** shows the SrO segregation on the LSCF surface as a function of temperature after aging in synthetic air for 25 hours. The Sr-rich nature of the particles was verified

through EDS measurements **(Figure S1)**. It is noted that similar studies in scope and methodology have not reported initial cation segregation upon sintering, possibly due to higher thermodynamic stability of the perovskite structure relative to SrO_x at such high temperatures or short sintering time.[25,32] This is verified by our XPS data for the unaged sample **(Figure S6)**. These studies have also reported SrO formation under the aging conditions in which we tested. The formation of $SrCO_3$ is ruled out due to the lack of a significant amount of CO_2 (beyond ppm contaminant levels) in the N_2 and O_2 testing gas environments, when CO_2 was not a feed gas.

No SrO is detected for the sample aged at 500°C **(Figure 1 (A))**, and above 600°C, SrO particles start to form, indicating that thermal energy is one of the key factors that determines segregation kinetics. These particles tend to agglomerate at higher temperatures. Above 800°C **(Figure 1 (E))**, some grains exhibited pores that grow with increasing temperature, and the degree of porosity is dependent on crystalline grain orientation. The same behavior is observed for the sample aged at 850°C **(Figure S2)**. Similar increases in surface roughness and pores have been observed elsewhere but are not discussed in detail.[22,33–35] These pores were likely formed by Sr diffusing out of the lattice in large quantities and leaving behind pores. It appears that the grain orientation determines the roughness of these grains, suggesting that grains terminated with a Sr plane may allow more Sr to diffuse out of these grains. The surface morphology of an as sintered LSCF sample (1400°C) is shown in **Figure 1 (F)**. The grain boundaries are clearly seen because of the thermal etching, and no SrO segregation is observed. It suggests that LSCF is relatively stable at high temperature, and the SrO segregation tends to occur in a specific temperature window.

The particle size and surface Sr coverage as a function of temperature is summarized in **Figure 1 (G)**. The precipitated particle distribution at different temperatures is determined using image analysis, as shown in **Figure 1 (H)**. Temperature significantly affects the precipitated SrO

particle size and quantity. When aged at 600°C, the average particle size is about 60 nm in diameter. The increase in temperature thermally activates surface Sr diffusion and promotes the agglomeration of segregated particles. However, the surface Sr coverage decreases at 800°C, compared to the one at 700°C, as a result of the vertical growth of SrO particles to lower the surface energy. The trend of increasing particle size but not surface coverage with temperature, as seen in **Figure 1 (G)**, suggests Ostwald ripening above 700°C. As a result of these pores and the high level of surface coverage, particle size distribution was not done above 800°C.

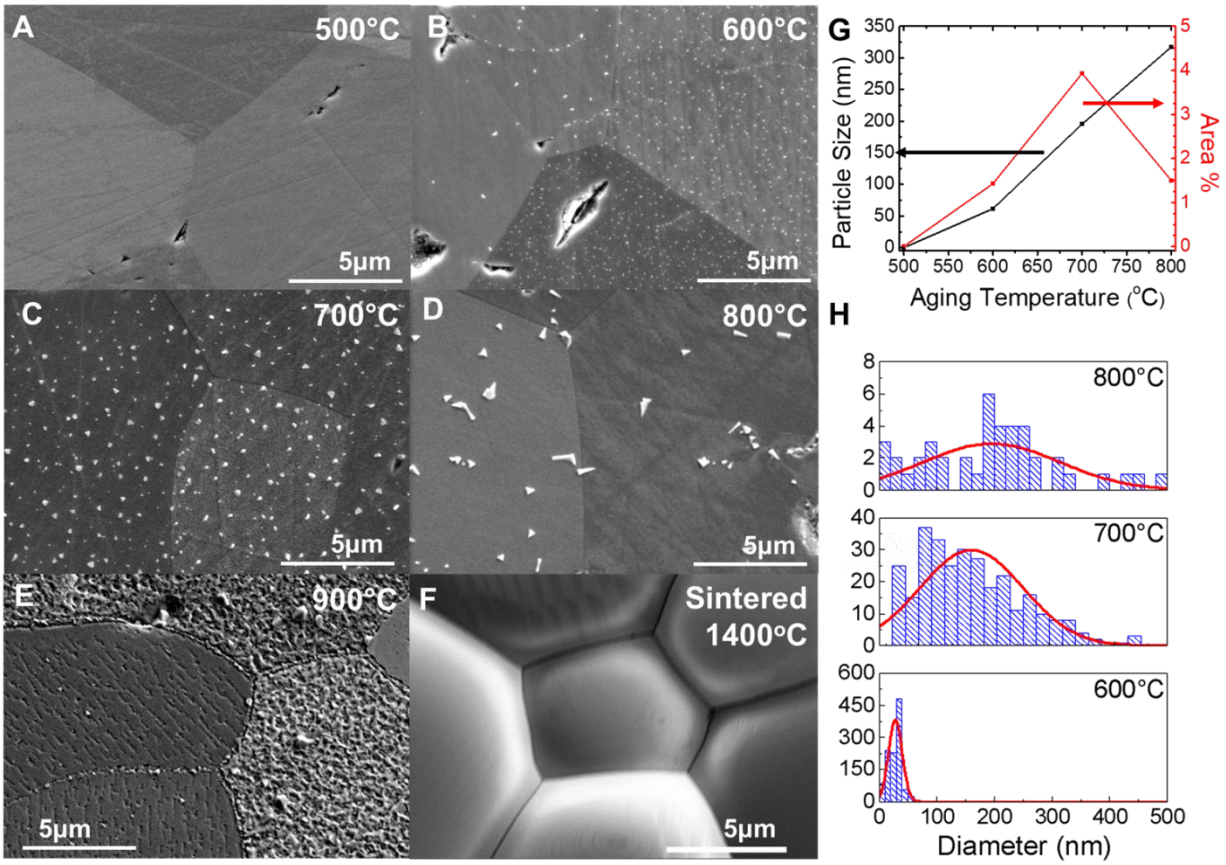

Figure 1. Temperature Effect on LSCF Cation Segregation. LSCF dense samples were aged for 25 hours in synthetic air at (A) 500°C, (B) 600°C, (C) 700°C, (D) 800°C, and (E) 900°C. (F) Sintered surface microstructure (G) Average particle size and surface coverage as a function of temperature (H) Particle size distribution at each temperature

Dense LSCF samples were aged at 700°C for different amounts of time to determine the cation segregation kinetics, **Figure 2 (A-D)** shows the LSCF surface. The amount of surface covered by particles appears to increase significantly in the first 25 hours and subsequently plateau with further aging. As expected, no secondary phase in the unaged sample can be seen on the pristine surface, **Figure 2 (E)**. Aging time also appears to increase the maximum particle size and the quantity of particles as shown in the particle size and surface Sr coverage plot in **Figure 2 (F-G)**. A similar trend in aging time in air was reported by Niania *et al.*,[25] in which there was a local minimum in surface area coverage, albeit under different temperatures and pressures. The local minimum at 50 hours may be attributed to Oswald ripening, which also occurs with increasing temperature, leading to vertical growth of the larger particles and thus less surface coverage.

In addition, grain boundaries became easier to distinguish after aging even when no SrO segregation was observed, which may be the result of thermal etching caused by Sr diffusion through the grain boundaries. Finally, it can also be seen that some grains stand out relative to their neighbors, exhibiting either more numerous smaller particles or fewer larger particles. This is especially clear at 75 hours, **Figure 2 (C)**. The effect of grain orientation on secondary phase formation has been observed in other works and is attributed to different defect formation energies for each grain orientation.[23]

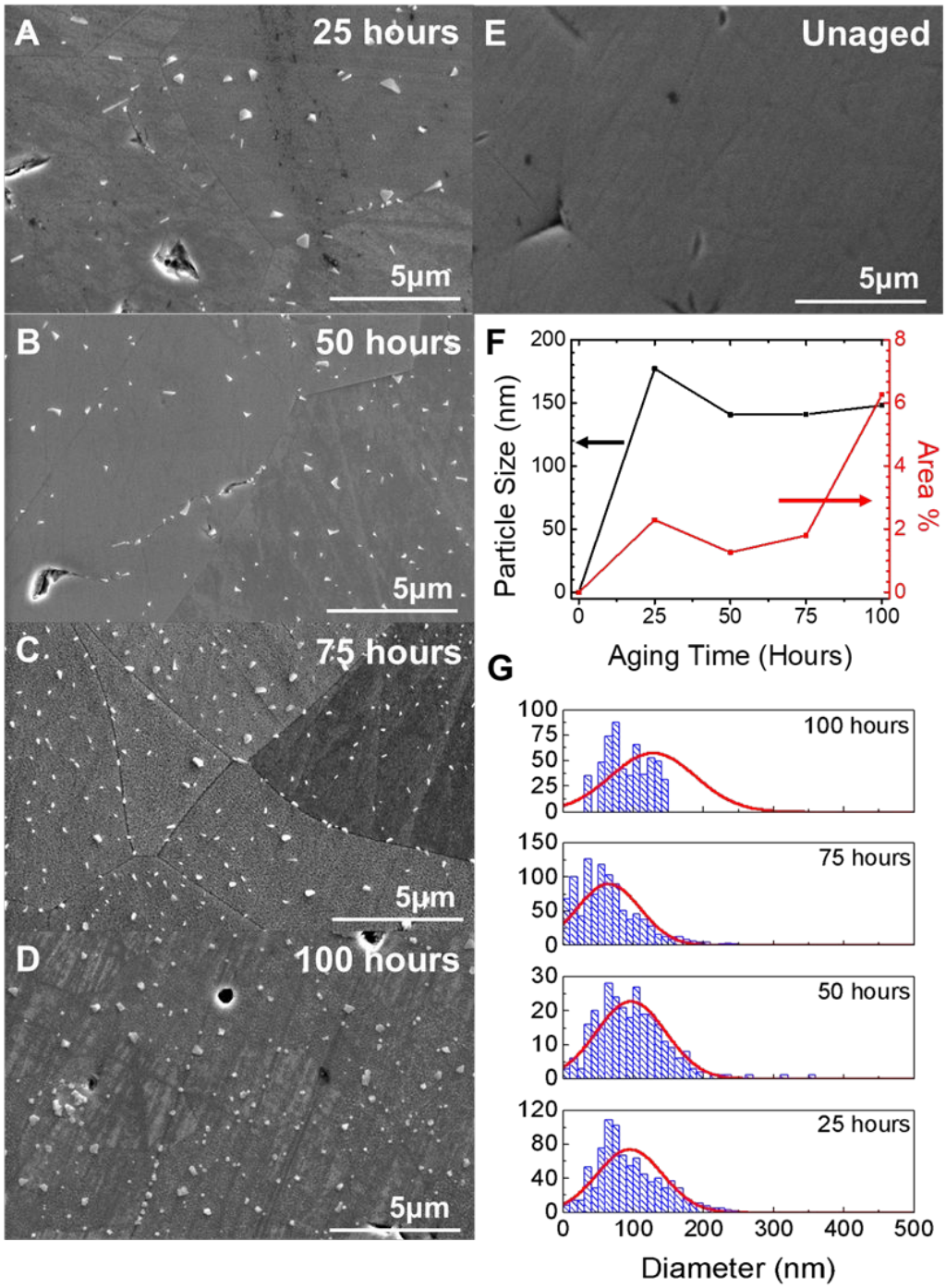

Figure 2. Aging Time Effect on LSCF Cation Segregation at 700°C. Dense LSCF samples were aged at 700°C for (A) 25, (B) 50, (C) 75, and (D) 100 hours in synthetic air. (E) Unaged polished sample (F) Average particle size and surface coverage of SrO as a function of aging time. (G) Particle size distribution as a function of time.

To observe effects of gas composition on the surface cation segregation of LSCF, 700°C was chosen as the temperature of interest because temperature effects dominate the surface precipitation above 800°C and the kinetics are too slow below 600°C. The pO_2 effects on the LSCF surface are shown in **Figure 3**. The increase in pO_2, **Figure 3 (A-D)**, shows that the amount of SrO particles reaches a maximum at pO_2=0.21 atm, **(Figure 3 (B))**. In 100 % N_2, there were no observable SrO particles on the LSCF surface **(Figure 3 (E))**. Thus, the lack of available oxygen molecules prevents the nucleation of surface particles. This suggests that without oxygen molecules, Sr nucleation and agglomeration into particles is severely hindered. On the other hand, higher pO_2 (0.5 and 1 atm) did not necessarily create more secondary phase as seen in **Figure 3 (F-G)**.

The particle size distribution in different pO_2's is shown in **Figure 3 (G)**. The change in pO_2 level directly impacts the size and quantity of SrO segregation. Both the particle size and the Sr surface coverage first increase and then decrease with the increase in pO_2, as shown in **Figure 3 (F)**. Niania et al.[25] also observed that SrO segregation on LSCF is more pronounced in air than pure O_2, and they conclude that either H_2O or CO_2 in air is likely the main cause. However, their observations were done in a low-pressure environment possibly influencing the degree of contribution from gas-phase impurities. On the other hand, our results are based on a controlled gas environment where the impurity level of H_2O and CO_2 were clearly accounted for, indicating that pO_2 is the main cause. This pO_2 dependence has a peak around pO_2=0.21 atm. This suggests that pO_2 modulates cation segregation and SrO nucleation through multiple mechanisms, which could be the combination of the surface nucleation mechanism or the electrostatic potential that are generated between surface and bulk.[36,37]

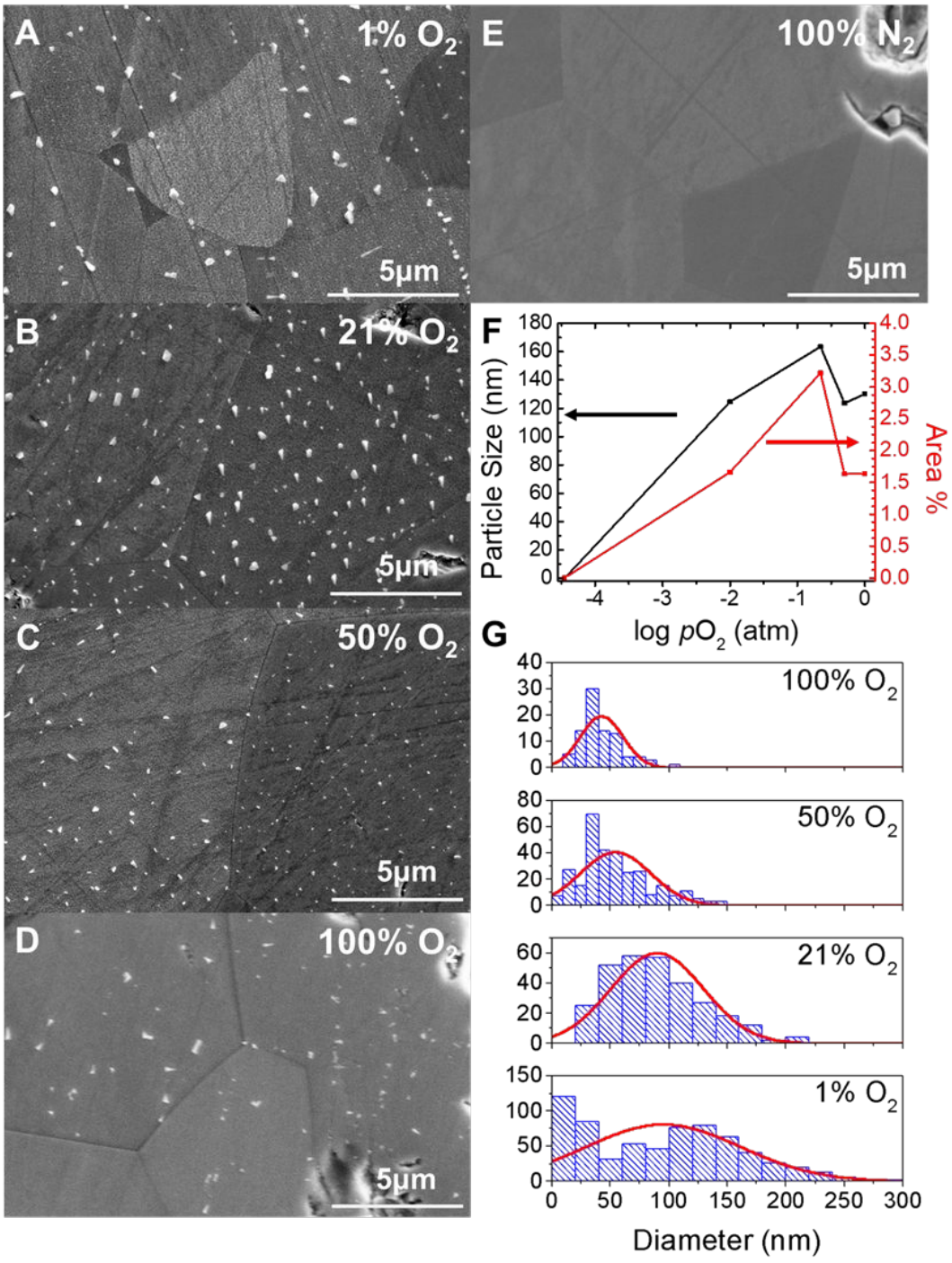

Figure 3. pO_2 Effect on LSCF Cation Segregation. LSCF dense samples were aged at 700°C for 25 hours in (A) 1% O_2 (B) 21% O_2 (C) 50% O_2 (D) 100% O_2 (E) 100% N_2. (F) SrO Particle size distribution with different pO_2's. (G) Particle size and surface coverage of SrO as a function of log pO_2.

The surface composition after aging LSCF in different gas environments was determined using XRD, **(Figure S3)** and Raman Spectroscopy **(Figure S4)** but did not show significant changes in nearly all aging environments. The XPS Sr 3d spectra of aged LSCF and fresh LSCF were shown in **Figure 4 (A)**, and corresponding table **Figure S6**. Peaks of Sr within the bulk of LSCF lattice along with surface segregated Sr are shown in green and blue, respectively. The peak intensities of these two species have a strong dependence on gas environment. The high intensities of surface segregated Sr peaks indicate that the surface segregation is more severe at that testing condition. We used the ratio of those characteristic peaks to quantify the degrees of surface segregation as a function of pO_2, as shown in **Figure 4 (C)**, respectively. The black line in the plot represents the ratio for the baseline sample (fresh, unaged LSCF). Samples aged in 20% and 50% O_2 show the highest degree of SrO segregation, which is consistent with the observation from SEM morphologies.

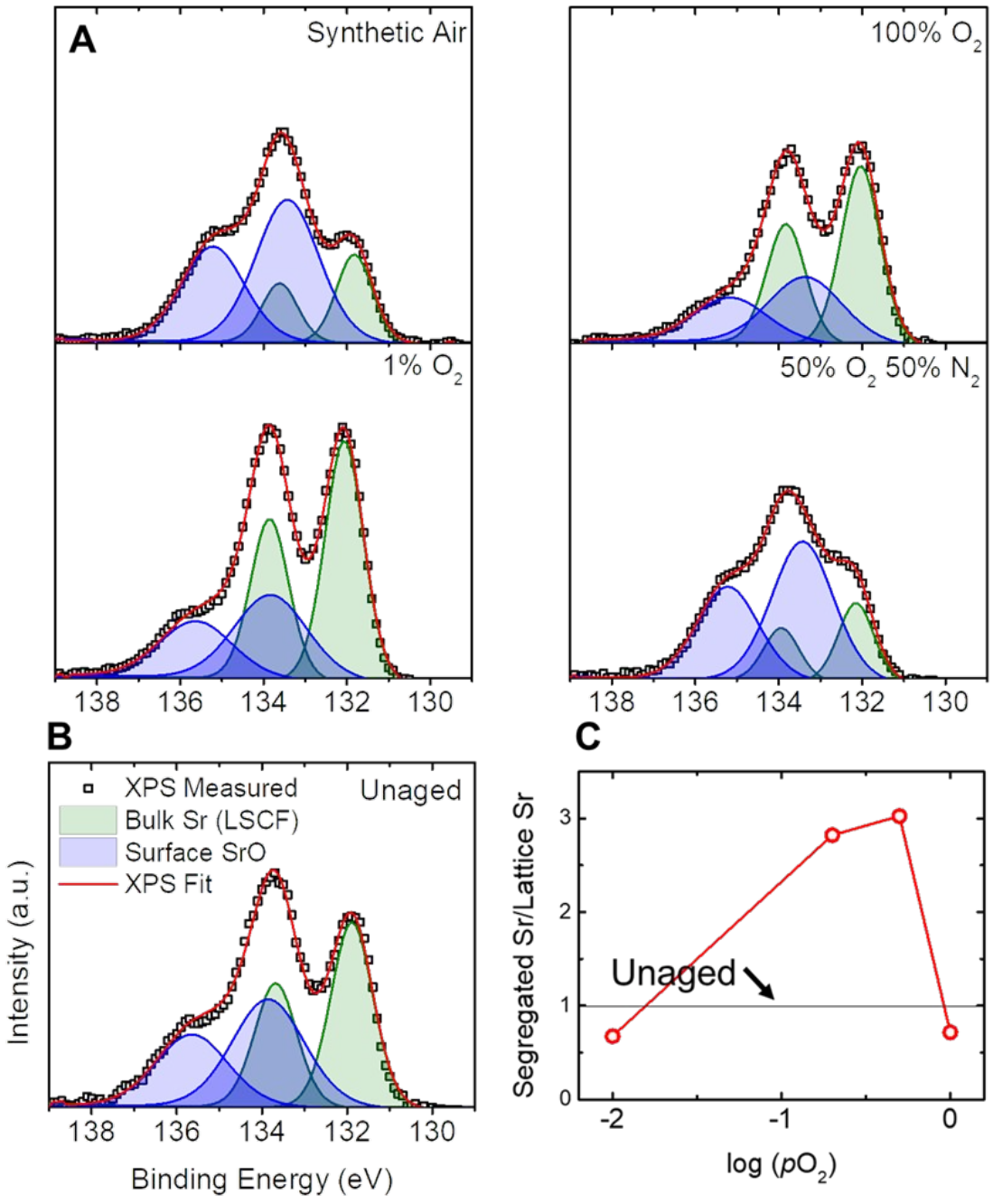

Figure 4. Environment Effects on Surface Chemistry of LSCF. XPS of Sr 3d spectra in (A) Different O_2 environments and (B) pristine LSCF. LSCF lattice Sr peaks are shown in green and surface segregated Sr peaks are shown in blue. (C) The ratio of surface segregated Sr and Sr in LSCF lattice as a function of O_2. LSCF samples were aged at 700°C for 25 hours in the listed environment.

Figure 5 shows the LSCF surface evolution with varying pCO_2 and corresponding particle size analysis and distribution curves. As the pCO_2 increases from its ambient air value (200-400ppm) to 80% CO_2 **(Figure 5 (A-F))**, the particle size decreases, except in an O_2 free environment **(Figure 5 (F))**. Note that the formation of SrO particles aligns at scratches created during sample polishing, suggesting that the defects on the surface are active nucleation sites for Sr segregation, which is consistent with results observed by Niania et al.[25] The particle size as a function of pCO_2 is shown in **Figure 5 (G)**, where an inverse relationship is observed between pCO_2 concentration and the particle size. It suggests that CO_2 not only promotes the nucleation of SrO but also limits the surface diffusion, or agglomeration, of SrO. The open symbol denotes CO_2 aged samples in 80% CO_2 /20% N_2 (without O_2). In this case, the particles are considerably larger **(Figure 5 (F))**. This implies that even when O_2 molecules are absent in the system, the presence of oxygen-containing CO_2 promotes the growth of surface strontium carbonates. Theoretical calculation results also suggest high stability of $SrCO_3$ in low pO_2 environments.[38,39]

When CO_2 is present, together with O_2, both SrO and $SrCO_3$ phases may form on the surface since both are stable under the testing conditions.[40] The presence of CO_2 promotes the formation of $SrCO_3$, which facilitates the SrO segregation process. Note that once CO_2 is removed, $SrCO_3$ tends to release CO_2 and form SrO. The morphology of the surface particles may be explained by SrO passivated with $SrCO_3$ rather than distinct particles of one or the other. Such a scenario is reported in Yu et al.[41] One study on aging LSCF in the presence of CO_2 showed that the LSCF surface Sr segregation became self-limiting in the presence of CO_2, reaching a steady state only when CO_2 was present.[42] Thus it is hypothesized that a carbonate layer is formed on the nucleating SrO particles once CO_2 is present, and as the SrO surface is passivated by CO_2, the agglomeration process is subsequently limited. However, CO_2 generally increases the number of

particles, suggesting that CO_2 only interacts with segregated Sr rather than the whole surface, blocking agglomeration but not nucleation. The area coverage relationship is less straightforward compared to the one between area coverage and pO_2 but suggests that despite the massive increase in the quantity of particles, their smaller size does not lead to total surface coverage. This is seen in **Figure 5 (G)**; the drop in area coverage from 50% CO_2 to 80% CO_2 may be due to particles too small to be quantified. The SrO particle size distribution as a function of CO_2 concentration is summarized in **Figure 5 (H)**, and the presence of CO_2 decreases the particle size from over 200 nm to 50 nm, and the quantity of particles increases from tens to thousands. XPS studies of LSCF aged in CO_2, **Figure S5**, show that SrO signals are higher than baseline **(Figure 4 (B))**, suggesting that the presence of gaseous CO_2 molecules actively interact with the surface Sr of LSCF. It is also worth mentioning that despite the much larger particle size observed in the 80% CO_2 with N_2 sample, the 80% CO_2 with O_2 shows a higher degree of Sr segregation according to XPS. The larger particle size may be attributed to the increased stability of $SrCO_3$ in low pO_2 environments.[38,39]

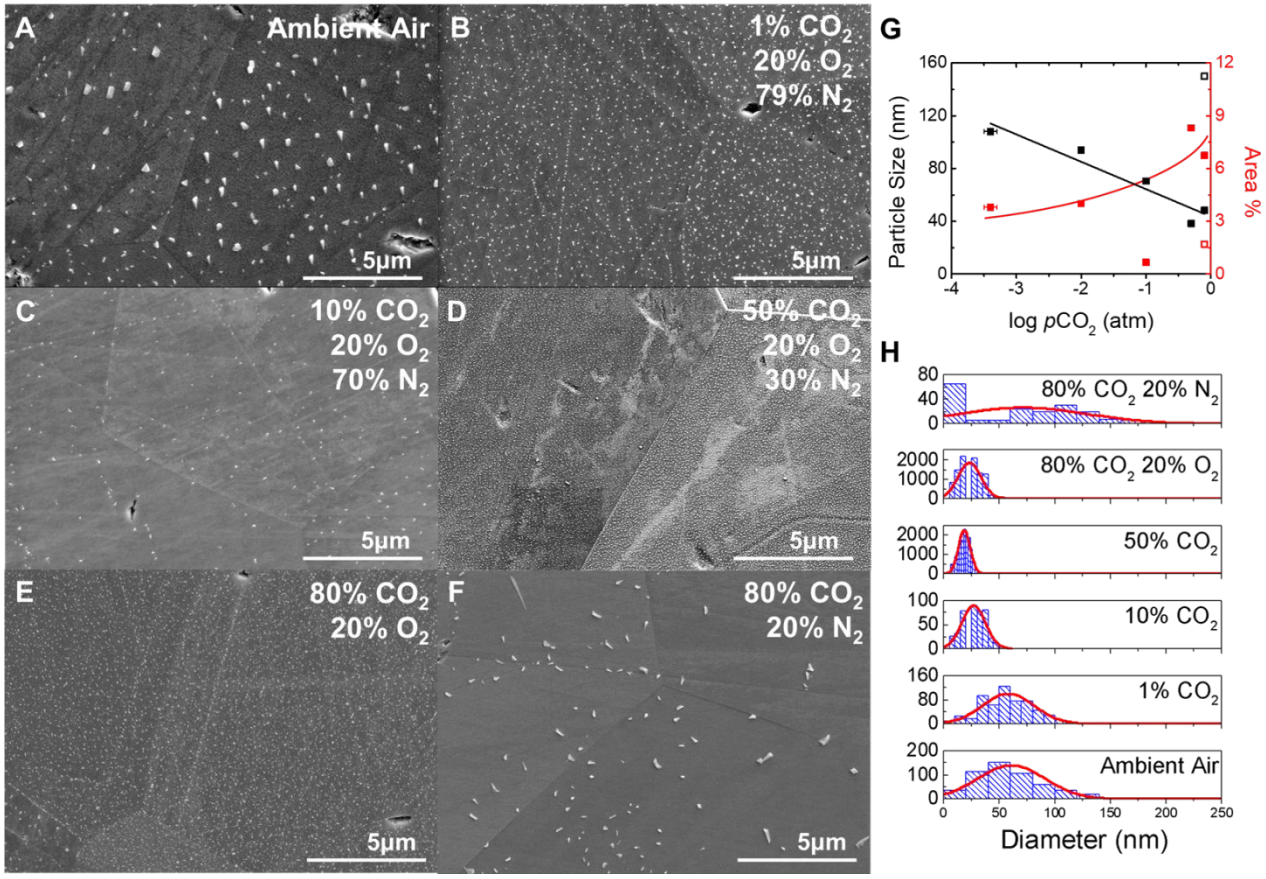

Figure 5. pCO_2 Effect on LSCF Cation Segregation. LSCF dense samples were aged at 700°C for 25 hours in (A) Ambient air, (B) 1 % CO_2 /20% O_2, (C) 10% CO_2 /20% O_2 (D), 50% CO_2 /20% O_2, (E) 80% CO_2 /20% O_2 and (F) 80% CO_2 /20% N_2. (G) Particle size (nm) and particle quantity (#) as a function of log pCO_2. (H) SrO Particle size distribution as different pCO_2's.

To understand the A-site stoichiometry effect on cation segregation, A-site deficient $(La_{0.6}Sr_{0.4})_{0.95}Co_{0.2}Fe_{0.8}O_3$ (LSCF095) was also aged in the same conditions as the stoichiometric LSCF. The surface morphologies of aged LSCF095 in different pO_2 and pCO_2 environments is shown in **Figure 6**. The deficiency in A-site stoichiometry of LSCF successfully suppresses SrO segregation in different pO_2's, as shown in **Figure 6 (A-B)**, compared to stoichiometric LSCF in **Figure 5**. This suggests that the presence of O_2 and available Sr cations on the surface are needed to initiate SrO nucleation. However, A-site deficiency shows no effect on CO_2 induced cation

segregation compared to A-site stoichiometric LSCF, as shown in **Figure 6 (C),** and the enlarged view in **Figure 6 (D)**. This evidence shows that gaseous CO_2 molecules actively promote SrO nucleation.

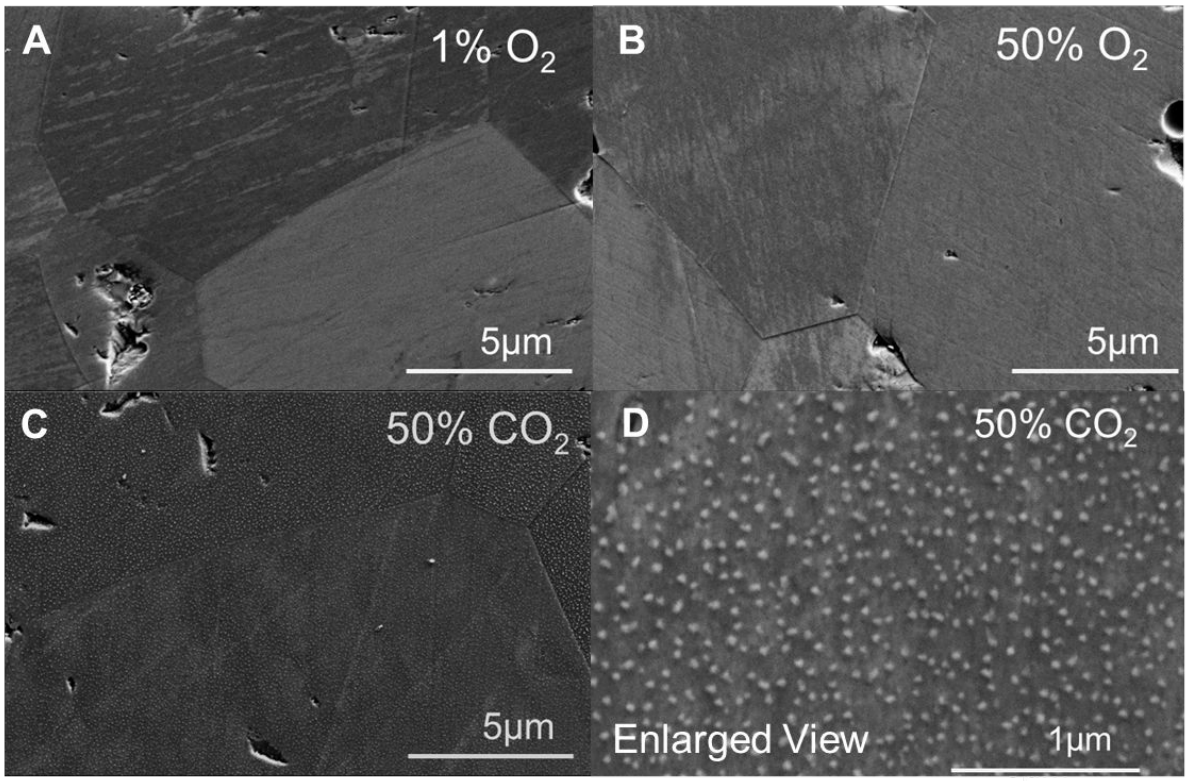

Figure 6. A-site stoichiometry effect on LSCF Cation Segregation. A site deficient $(La_{0.6}Sr_{0.4})_{0.95}Co_{0.2}Fe_{0.8}O_3$ LSCF095 dense samples were aged at 700°C for 25 hours in (A) 1%O_2, (B) 50% O_2, (C) 50%CO_2 (balanced with 20% O_2, 30%N_2) with (D) a higher magnification.

Among all the tested variables, temperature (for T ≤ 800°C) and time most clearly affect the level of SrO segregation since both thermodynamics and kinetics favor cation segregation. In addition, the gas environments such as pO_2 and pCO_2 play a vital role in the cation segregation process. The change in pO_2 alters the oxygen potential at the LSCF surface and is expected to cause a difference in oxygen stoichiometry and lattice strain. To identify the possible driving force, elastic strain and electrostatic interactions, for the segregation, we investigated the changes in non-

stoichiometry and lattice constant of LSCF as a function of temperature and pO_2. **Figure 7 (A)** shows pO_2 effects on LSCF lattice constant at different temperatures as reported by Fukuda et al.[46], and the SrO segregation level at 700°C as a function of pO_2 is also shown. The lattice constant of LSCF increases as pO_2 decreases because of chemical expansion, and this expansion is expected to induce contraction strain in the lattice. The SrO segregation level increases as pO_2 increases from N_2 to synthetic air environment; however, once pO_2 increases above air level (0.21 atm), the SrO segregation level decreases. This conflicting dependency suggests that the elastic strain might not be the main segregation driving force.

Figure 7 (**B**) shows oxygen non-stoichiometry (δ) as a function of pO_2 on the basis of experimental results reported by Fukuda et al.[47], Kuhn et al.[48], and Stevenson et al.[49]. The ranges of δ values at 600°C, 700°C, and 800°C are highlighted in black, red, and blue color bands. The non-stoichiometry of LSCF affects space charge (electrostatic energy), and we can match up samples tested at different conditions but with a similar δ to test the hypothesis of the electrostatic energy as the main driving force. This figure indicates that the sample aged at 800°C in synthetic air has a similar δ as the one aged at 700°C between $pO_2=10^{-2}$ and 10^{-4} atm. However, these samples yield different degrees of segregation, suggesting that the difference in δ might also not be directly related to the main driving force.

We show that gaseous oxygen-containing molecules, solid-state defect chemistry of oxides, and the surface free energy are the three main factors controlling the segregation level. **Figure 7** (C) shows the proposed mechanism behind Sr surface segregation. The intensive variables, temperature and pO_2, control the thermodynamic status of segregation. At low temperature (<500°C), insufficient thermal energy limits segregation kinetics. In contrast, at high temperature

(1400°C), no cation segregation is observed mainly because the free energy of La-Sr-Co-Fe-O in perovskite phase is lower.

The presence of oxygen-containing molecules at the surface creates an oxygen chemical potential between the bulk and surface causing a driving force for ion diffusion. These surface molecules also act as reactants, interacting with diffused Sr cations and nucleating at the surface. In the high pO_2 case, it is hypothesized that higher pO_2 reduces surface particle growth because of the defect chemistry. At higher pO_2's with a lower δ value, higher concentration of lattice oxygen stabilizes lattice Sr through coulombic interactions. This stabilizing effect, as reported by Ding et al.[24] and Oh *et al.*,[7] would explain the reduced particle formation. After nucleation, SrO moves freely on the surface and tend to agglomeration into larger particles.

Once CO_2 is present, the particle size of segregated SrO decreased dramatically. Experiments on LSF and LSCF suggest that CO_2 passivates their surface and block reactions. In this scenario it is likely that $SrCO_3$ forms as transient intermediate $SrCO_3$ as shown in **Figure 7 (D).**[39,42] Since CO_2 preferably adsorbs onto the Sr sites, it creates the oxygen chemical potential at the surface and promotes the nucleation process through the formation of carbonates. These intermediate carbonates tend to limit the surface migration of Sr-containing species, causing the isolated particles.

Note that this study was performed under no external electrochemical driving force. Once electrochemical potentials are presented, the overpotential drop across cathode surface could significantly changes its surface structure and composition,[50–53] which may enhance the interactions between the cathode surface and gases and further induce cation segregation. Thus, applying an electrochemical potential presents an additional opportunity for further study of the driving forces for cation segregation.

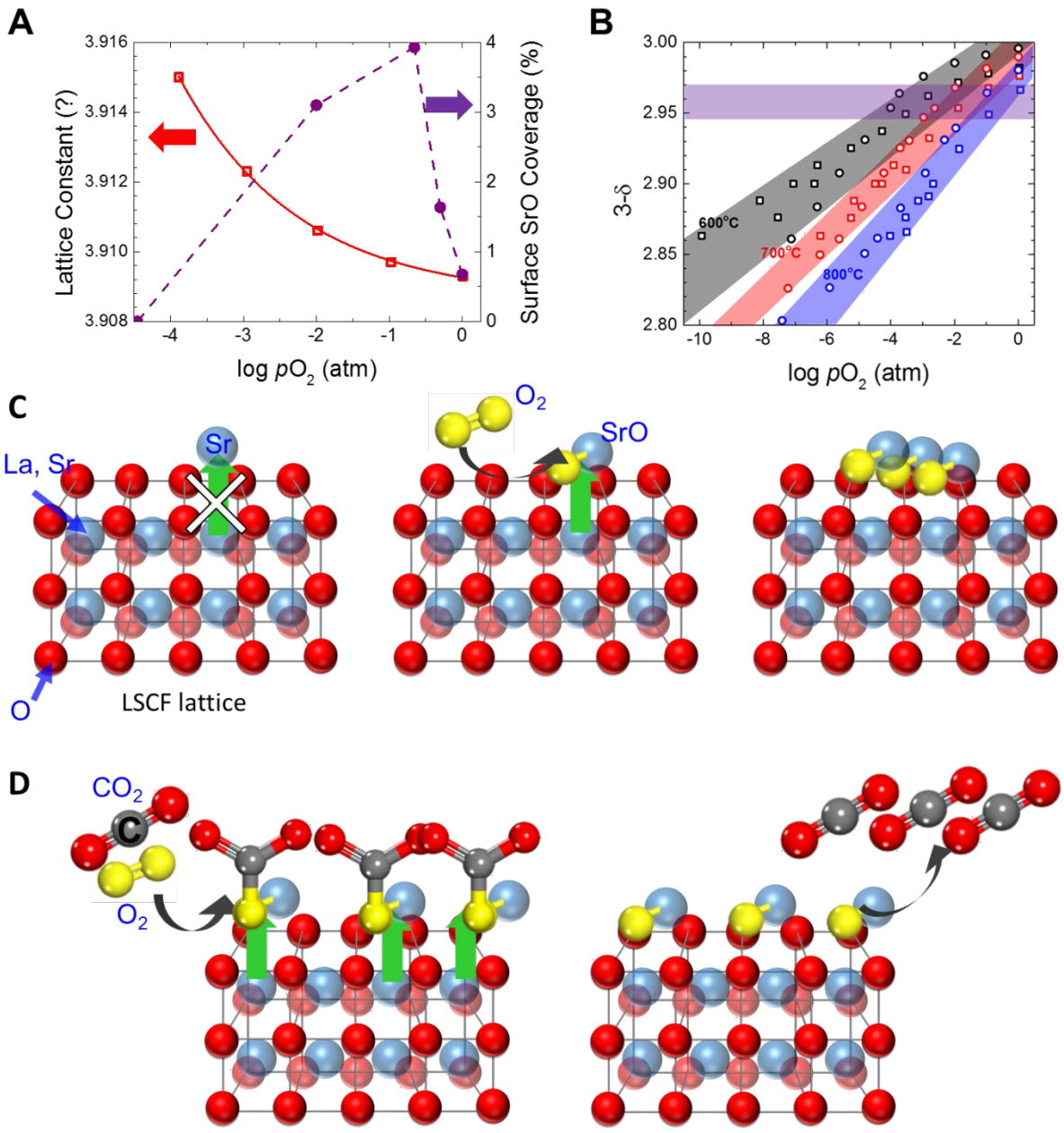

Figure 7. Possible Driving Forces and Cation Segregation Mechanism. (A) lattice constant and surface coverage as a function of pO_2. The red square shows the lattice constant of LSCF.[46] The purple circle symbols represent SrO surface coverage of LSCF aged at 700°C in different pO_2's for 25 hours. (B) Non-stoichiometry as a function of pO_2. The color bands represent different oxygen stoichiometry zone of LSCF at different temperatures. The region highlighted in purple is the oxygen stoichiometry of interest (δ =0.03~0.06), which are achieved at 800°C in synthetic air or at 700°C between pO_2 =10^{-1}~10^{-4} atm. (C) O_2 and CO_2 effect on nucleation. Sr diffusion is mitigated once no oxygen-containing gaseous species are present. SrO nucleation occurs once O_2 is present, promoting the diffusion, nucleation, and

eventually agglomeration. (D) O_2 and CO_2 effect on growth. Carbonates are formed with the presence of CO_2, which limit the surface migration.

Conclusion

The LSCF surface microstructure after aging was found to vary greatly based on aging conditions of temperature, aging time, pO_2, and pCO_2. As expected, increased temperature and aging time promote surface SrO segregation, with the overall trends suggest Ostwald ripening. The underlying grain orientation appeared to impact the degree of segregation. In addition to the formation of SrO particles, sufficiently high temperatures cause coarsening of the SrO particles and form pores on the surface as a result of Sr diffusing out of the lattice.

A volcano-like trend in SrO segregation as a function of pO_2 is observed on LSCF, which is shown to be stable in a pure O_2 or inert environment, such as N_2. Lack of O_2 reactants at low pO_2 and the low oxygen vacancy concentration at high pO_2 are likely the causes of the decrease in SrO segregation level. Unfortunately, maximum SrO segregation occurs at around the pO_2 of air.

Meanwhile gaseous impurities also affect SrO particle nucleation. The size of segregated particles shows a direct correlation with pCO_2, as the formation of surface carbonates intermediate species limit the surface mobility. increase in CO_2 seems to affect the mechanism of SrO aggregation while promoting SrO precipitation. The presence of CO_2 in the environment may cause preferential formation of $SrCO_3$ rather than SrO, and this $SrCO_3$, if formed, does not agglomerate to the same extent as SrO. A-site deficiency can limit SrO segregation, but once CO_2 is present, A-site deficiency has little to no effect on preventing cation segregation. This analysis of such a wide range of aging conditions for LSCF should promote future developments in the stability of cathode materials.

Experimental Section

Material Preparation: Dense samples were made by pressing commercially available $La_{0.6}Sr_{0.4}Co_{0.2}Fe_{0.8}O_3$ (LSCF) and $(La_{0.6}Sr_{0.4})_{0.95}Co_{0.2}Fe_{0.8}O_3$ (LSCF095) powder (Praxair) with a hydraulic press. The resulting discs were sintered in air at 1400°C for 4 hours for LSCF. Once sintered, the discs were polished with SiC sandpaper down to 8μ and then polished with diamond polishing particles to 0.25μ. This enables observation of grain boundaries with SEM. The polished samples were aged in environmentally controlled reactors. Gas flow rates were controlled with mass flow controllers and the gas environment was verified with a Zirox SGM5EL pO_2 sensor. The gases O_2, N_2, CO_2, and H_2 (Airgas, ultra-high purity) were used to create each testing environment.

Characterization: The surface morphology is monitored using scanning electron microscopy (SEM), and the precipitated particle size and distribution are further quantified through image analysis. After aging conditions were met, the surface of each sample was studied using a Hitachi Su70 SEM. The subsequent images were then analyzed using ImageJ. The Trainable WEKA Segmentation plugin for ImageJ was used to distinguish between the background and particles. The resulting image could then be quantified to determine the particle frequency and size distribution. An analysis of the surface particles was then carried out using ImageJ software and the Trainable WEKA Segmentation plugin (WEKA).[54] An example of this process is shown in **Figure S7.** Particle phase and surface phases were studied with a Bruker D8 powder X-ray diffractometer (XRD) with Cu Kα radiation. Raman spectroscopy was performed using an Yvon Jobin LabRam ARAMIS confocal Raman microscope.

Acknowledgments

Authors wish to acknowledge the support of the U.S. Department of Energy, NETL, Contract #: DEFE0031662.

References

1. Wachsman, E. D. & Lee, K. T. Lowering the temperature of solid oxide fuel cells. *Science* **334**, 935–939 (2011).
2. Xia, C., Rauch, W., Chen, F. & Liu, M. Sm0.5Sr0.5CoO3 Cathodes for Low-Temperature SOFCs. *Solid State Ionics* **149**, 11–19 (2002).
3. Kharton, V. V *et al.* Perovskite-type oxides for high-temperature oxygen separation membranes. *Journal of Membrane Science* **163**, 307–317 (1999).
4. Harrison, W. A. Origin of Sr segregation at La 1 − x Sr x MnO 3 surfaces. **155437**, 1–5 (2011).
5. Seob, H., Min, J., Kim, J. & Moon, J. Phase stability of Sm0.5Sr0.5CoO3 cathodes for on-planar type, single-chamber, solid oxide fuel cells. *Journal of Power Sources* **191**, 269–274 (2009).
6. Li, Y. *et al.* Controlling cation segregation in perovskite-based electrodes for high electro-catalytic activity and durability. *Chemical Society Reviews* **46**, 6345–6378 (2017).
7. Oh, D., Gostovic, D. & Wachsman, E. D. Mechanism of La0.6Sr0.4Co0.2Fe0.8O3 cathode degradation Dongjo. *Journal of Materials Research* **27**, 1992–1999 (2012).
8. Chen, H. *et al.* Improving the Electrocatalytic Activity and Durability of the La0.6Sr0.4Co0.2Fe0.8O3-δ Cathode by Surface Modification. *ACS Applied Materials and Interfaces* **10**, 39785–39793 (2018).
9. Jung, W. & Tuller, H. L. Investigation of surface Sr segregation in model thin film solid oxide fuel cell perovskite electrodes. *Energy and Environmental Science* **5**, 5370–5378 (2012).

10. Huang, Y., Hussain, A. M., Pellegrinelli, C., Xiong, C. & Wachsman, E. D. Chromium Poisoning Effects on Surface Exchange Kinetics of La0.6Sr0.4Co0.2Fe0.8O3-d. *ACS Applied Materials and Interfaces* **9**, 0–8 (2017).
11. Soldati, A. L. *et al.* Degradation of oxygen reduction reaction kinetics in porous La0.6Sr0.4Co0.2Fe0.8O3-d cathodes due to aging-induced changes insurface chemistry. *Journal of Power Sources* **337**, 166–172 (2017).
12. Simner, S. P., Anderson, M. D., Engelhard, M. H. & Stevenson, J. W. Degradation mechanisms of La-Sr-Co-Fe-O3 SOFC cathodes. *Electrochemical and Solid-State Letters* **9**, 478–481 (2006).
13. Liu, Y. *et al.* Performance stability and degradation mechanism of La0.6Sr0.4Co0.2Fe0.8O3-δ cathodes under solid oxide fuel cells operation conditions. *International Journal of Hydrogen Energy* **39**, 15868–15876 (2014).
14. Yan, A., Maragou, V., Arico, A., Cheng, M. & Tsiakaras, P. Investigation of a Ba0.5Sr0.5Co0.8Fe0.2O3-δ based cathode SOFC. II. The effect of CO2 on the chemical stability. *Applied Catalysis B: Environmental* **76**, 320–327 (2007).
15. Zhao, Z. *et al.* High and low temperature behaviors of La0.6Sr 0.4Co0.2Fe0.8O3-δ cathode operating under CO2/H2O-containing atmosphere. *International Journal of Hydrogen Energy* **38**, 15361–15370 (2013).
16. Hu, B., Mahapatra, M. K., Keane, M., Zhang, H. & Singh, P. Effect of CO2 on the stability of strontium doped lanthanum manganite cathode. *Journal of Power Sources* **268**, 404–413 (2014).

17. Benson, S. J., Waller, D. & Kilner, J. A. Degradation of La0.6Sr0.4Fe0.8Co0.2O3-d in Carbon Dioxide and Water Atmospheres. *Journal of The Electrochemical Society* **146**, 1305–1309 (2000).
18. Wachsman, E. D., Huang, Y.-L., Pellegrinelli, C., Taillon, J. A. & Salamanca-Riba, L. G. Towards a Fundamental Understanding of the Cathode Degradation Mechanisms. *ECS Transactions* **61**, 47–56 (2014).
19. Huang, Y., Pellegrinelli, C., Sakbodin, M. & Wachsman, E. D. Molecular Reactions of O2 and CO2 on Ionically Conducting Catalyst. *ACS Catalysis* **8**, 1231–1237 (2018).
20. Huang, Y.-L. *et al.* Direct observation of enhanced water and carbon dioxide reactivity on multivalent metal oxides and their composites. *Energy and Environmental Science* **10**, 919–923 (2017).
21. Huang, Y., Pellegrinelli, C. & Wachsman, E. D. Oxygen Dissociation Kinetics of Concurrent Heterogeneous Reactions on Metal Oxides. *ACS Catalysis* **7**, 5766–5772 (2017).
22. Piskin, F., Bliem, R. & Yildiz, B. Effect of crystal orientation on the segregation of aliovalent dopants at the surface of La.Sr.CoO. *Journal of Materials Chemistry A* **6**, 14136–14145 (2018).
23. Chen, Y. *et al.* Segregated Chemistry and Structure on (001) and (100) Surfaces of (La 1 − x Sr x) 2 CoO 4 Override the Crystal Anisotropy in Oxygen Exchange Kinetics. *Chemistry of Materials* **27**, (2015).
24. Ding, H., Virkar, A. V, Liu, M. & Liu, F. Suppression of Sr surface segregation in La1-xSrxCo1-yFeyO3-d: a first principles study. *Physical chemistry chemical physics : PCCP* **15**, 489–496 (2013).
25. Mathew Niania, Renaud Podor, T. Ben Britton, Cheng Li, S. J. C. & Nikolai Svetkov, S. S. and J. K. In situ study of strontium segregation in La0.6Sr0.4Co0.2Fe0.8O3-d in ambient

atmospheres using high-temperature environmental scanning electron microscopy. *Journal of Materials Chemistry* **6**, 14120–14135 (2018).

26. Kwon, H., Lee, W. & Han, J. W. Suppressing cation segregation on lanthanum-based perovskite oxides to enhance the stability of solid oxide fuel cell cathodes. *RSC Advances* **6**, 69782–69789 (2016).
27. Araki, W., Miyashita, M. & Arai, Y. Strontium surface segregation in La0.6Sr0.4Co0.2Fe0.8O3−δ subjected to mechanical stress. *Solid State Ionics* **290**, 18–23 (2016).
28. Araki, W., Yamaguchi, T., Arai, Y. & Malzbender, J. Strontium surface segregation in La0.58Sr0.4Co0.2Fe0.8O3-δ annealed under compression. *Solid State Ionics* **268**, 1–6 (2014).
29. Orikasa, Y. *et al.* Surface strontium segregation of solid oxide fuel cell cathodes proved by in situ depth-resolved x-ray absorption spectroscopy. *ECS Electrochemistry Letters* **3**, F23–F26 (2014).
30. Wang, H. *et al.* Mechanisms of Performance Degradation of (La,Sr)(Co,Fe)O3-δ Solid Oxide Fuel Cell Cathodes. *Journal of The Electrochemical Society* **163**, F581–F585 (2016).
31. Rupp, G. M. *et al.* Surface chemistry of La0.6Sr0.4CoO3-δ thin films and its impact on the oxygen surface exchange resistance. *Journal of Materials Chemistry A* **3**, 22759–22769 (2015).
32. Oh, D., Gostovic, D. & Wachsman, E. D. Mechanism of $La_{0.6}Sr_{0.4}Co_{0.2}Fe_{0.8}O_3$ cathode degradation. *J. Mater. Res.* **27**, 1992–1999 (2012).
33. Oh, D., Yoo, J., Gostovic, D., Jones, K. & Wachsman, E. A Kinetic Study of Catalytic Activity Degradation of La0.6Sr0.4Co0.2Fe0.8O3-δ. *ECS Transactions* **16**, 97–105 (2009).

34. Zhao, L., Drennan, J., Kong, C. & Ping San, J. Insight into surface segregation and chromium deposition on La0.6Sr0.4Co0.2Fe0.8O3-d cathodes of solid oxide fuel cells. *Journal of Materials Chemistry A* **2**, 11114–11123 (2014).
35. Klande, T., Ravkina, O. & Feldhoff, A. Effect of A-site lanthanum doping on the CO2 tolerance of SrCo0.8Fe0.2O3-d oxygen-transporting membranes. *Journal of Membrane Science* **437**, 122–130 (2013).
36. Lee, Y. L., Kleis, J., Rossmeisl, J. & Morgan, D. Ab initio energetics of LaBO3 (001) (B=Mn, Fe, Co, and Ni) for solid oxide fuel cell cathodes. *Physical Review B - Condensed Matter and Materials Physics* **80**, 1–20 (2009).
37. Mebane, D. S. A variational approach to surface cation segregation in mixed conducting perovskites. *Computational Materials Science* **103**, 231–236 (2015).
38. Esposito, V., Søgaard, M. & Hendriksen, P. V. Chemical stability of La 0.6Sr 0.4CoO3-δ in oxygen permeation applications under exposure to N2 and CO2. *Solid State Ionics* **227**, 46–56 (2012).
39. Darvish, S., Zhong, Y. & Gopalan, S. Thermodynamic Stability of La0.6Sr 0.4Co0.2Fe0.8O3-δ in Carbon Dioxide Impurity: A Comprehensive Experimental and Computational Assessment. *ECS Transactions* **78**, 1021–1025 (2017).
40. Darvish, S., Gopalan, S. & Zhong, Y. Thermodynamic stability maps for the La0.6Sr0.4Co0.2Fe0.8O3±δ–CO2–O2 system for application in solid oxide fuel cells. *Journal of Power Sources* **336**, 351–359 (2016).
41. Yu, Y. *et al.* Effect of atmospheric CO2 on surface segregation and phase formation in La0.6Sr0.4Co0.2Fe0.8O3− thin films. *Applied Surface Science* **323**, 71–77 (2014).

42. Yu, Y. *et al.* Effect of atmospheric CO2 on surface segregation and phase formation in La0.6Sr0.4Co0.2Fe0.8O3-δ thin films. *Applied Surface Science* **323**, 71–77 (2014).

43. Lai, S. Y., Ding, D., Liu, M., Liu, M. & Alamgir, F. M. Operando and In situ X-ray Spectroscopies of Degradation in $La_{0.6}Sr_{0.4}Co_{0.2}Fe_{0.8}O_{3-\delta}$ Thin Film Cathodes in Fuel Cells. *ChemSusChem* **7**, 3078–3087 (2014).

44. Hardy, J. S. *et al. Effects of Humidity on Solid Oxide Fuel Cell Cathodes*. PNNL--24115, 1177304 http://www.osti.gov/servlets/purl/1177304/ (2015) doi:10.2172/1177304.

45. Shen, F. & Lu, K. Moisture Effect on La0.8Sr0.2MnO3 and La0.6Sr0.4Co0.2Fe0.8O3 Cathode Behaviors in Solid Oxide Fuel Cells. *Fuel Cells* **15**, 105–114 (2015).

46. Hashimoto, S. I. *et al.* Thermal and chemical lattice expansibility of La0.6Sr 0.4Co1-yFeyO3 - δ (y = 0.2, 0.4, 0.6 and 0.8). *Solid State Ionics* **186**, 37–43 (2011).

47. Kuhn, M. *et al.* Oxygen Nonstoichiometry and Thermo-Chemical Stability of Perovskite-Type La 0.6 Sr 0.4 Co 1- y Fe y O 3- δ (y = 0, 0.2, 0.4, 0.5, 0.6, 0.8, 1) Materials . *Journal of The Electrochemical Society* **160**, F34–F42 (2013).

48. Kuhn, M., Hashimoto, S., Sato, K., Yashiro, K. & Mizusaki, J. Oxygen nonstoichiometry, thermo-chemical stability and lattice expansion of La0.6Sr0.4FeO3-δ. *Solid State Ionics* **195**, 7–15 (2011).

49. Hardy, J. S., Templeton, J. W., Edwards, D. J., Lu, Z. & Stevenson, J. W. Lattice expansion of LSCF-6428 cathodes measured by in situ XRD during SOFC operation. *Journal of Power Sources* **198**, 76–82 (2012).

50. Baumann, F. S. *et al.* Strong Performance Improvement of La0.6Sr0.4Co0.8Fe0.2O3−□ SOFC Cathodes by Electrochemical Activation. *Journal of The Electrochemical Society* 7.

51. Finsterbusch, M., Lussier, A., Schaefer, J. A. & Idzerda, Y. U. Electrochemically driven cation segregation in the mixed conductor La0.6Sr0.4Co0.2Fe0.8O3−δ. *Solid State Ionics* **212**, 77–80 (2012).

52. Lu, M. Y. *et al.* Stable high current density operation of $La_{0.6}Sr_{0.4}Co_{0.2}Fe_{0.8}O_{3-\delta}$ oxygen electrodes. *J. Mater. Chem. A* **7**, 13531–13539 (2019).

53. Kim, D., Bliem, R., Hess, F., Gallet, J.-J. & Yildiz, B. Electrochemical Polarization Dependence of the Elastic and Electrostatic Driving Forces to Aliovalent Dopant Segregation on LaMnO3. *J. Am. Chem. Soc.* **142**, 3548–3563 (2020).

54. Arganda-carreras, I. *et al.* Trainable Weka Segmentation : a machine learning tool for microscopy pixel classification. *Bioinformatics* **33**, 2424–2426 (2017).

Table of Contents Entry

Effects of Surface Chemical Potentials on Cation Segregation

Yevgeniy Ostrovskiy,[a,b] Yi-Lin Huang, [a,b*] and Eric Wachsman [a,b*]

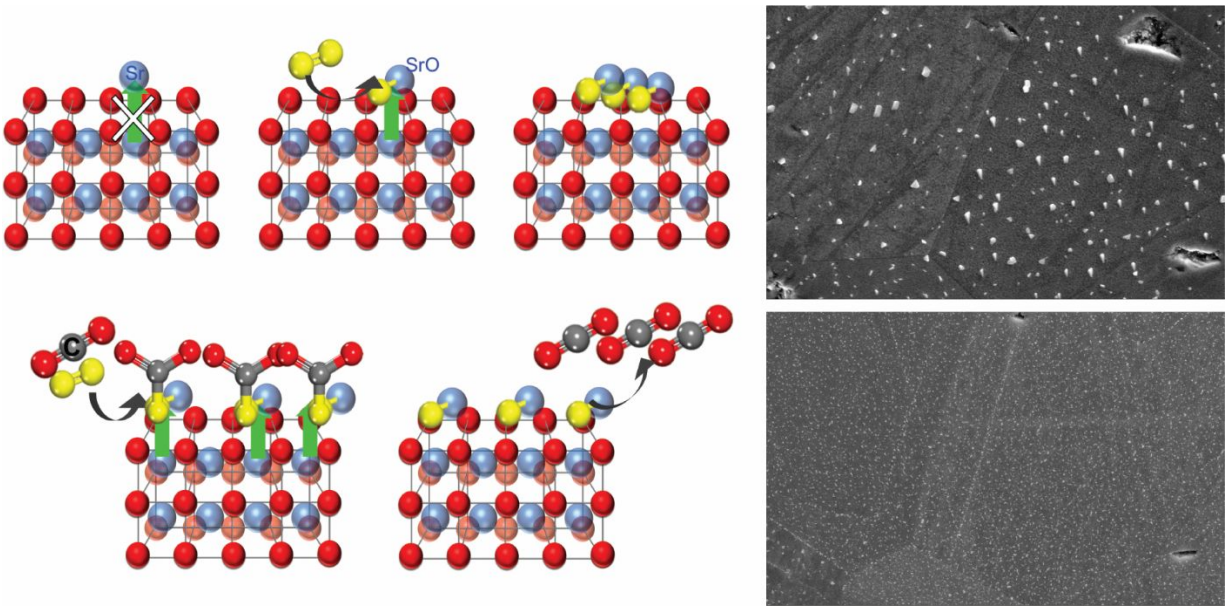

The presence of gas molecules alters the surface cation segregation process on perovskites.